Highly anharmonic potential modulation in lateral superlattices fabricated using epitaxial InGaAs stressors

R. J. Luyken,[a] A. Lorke,[b] A. M. Song, M. Streibl, and J. P. Kotthaus
Sektion Physik, LMU, Geschw.-Scholl Pl. 1, D-80539 München, Germany

C. Kadow, J. H. English, and A. C. Gossard
Materials Department and QUEST, University of California, Santa Barbara, California 93106

(Received 22 May 1998; accepted for publication 23 June 1998)

A coherently strained stressor structure is used to create a one-dimensional periodic potential in the two-dimensional electron gas at a AlGaAs/GaAs heterointerface. We demonstrate that from magnetotransport the Fourier coefficients of the conduction band modulation can be determined. In contrast to conventional electrostatic patterning, ''hard'' potential modulation with dominant contributions of higher harmonics is achieved. In the regime of narrow stressor-stressor distance, the strain-induced potential modulation can be calculated analytically from elasticity theory. The calculated magnetoresistance which can be derived from the stressor-induced potential is in good agreement with the experimental data. © *1998 American Institute of Physics.* [S0003-6951(98)03034-4]

With advances in miniaturization of semiconductor structures, the interplay between mechanical stress and electronic properties becomes more and more important. On the one hand, mechanical stress can limit the performance of small scale electronic devices. On the other hand, a controlled application of stress can be used to tailor the optical and electronic properties of semiconductor structures beyond common patterning techniques, such as etching or electrostatic modulation. Several optical investigations[1] have shown that patterned, stressed or strained films, so-called ''stressors,'' can be used to achieve nanoscale confinement with a relatively large band gap modulation. However, detailed information about the shape of the potential is difficult to obtain from optical experiments where mainly quantization effects in the potential minima are investigated. We show in the following that magnetotransport experiments can be used to probe the detailed shape of the potential.

It is now widely accepted that the dominant higher harmonics of the confining potential which were observed in some magnetotransport studies cannot be explained from electrostatic modulation alone, but arise from stress effects.[2–5] These higher harmonics can result in hard confining potentials which for some applications—e.g., quantum devices operating at elevated temperatures—are superior to conventional, essentially sinusoidal or parabolic potentials.

Here we report on magnetotransport measurements on a two-dimensional electron gas (2DEG) beneath an epitaxial stressor structure and apply a theory that allows us to determine the Fourier coefficients of the electronic potential at the location of the electron system. Contrary to conventional (e.g., evaporated or sputtered) strained structures, epitaxial stressors offer the possibility to accurately control the amount of stress during fabrication and allow for a precise theoretical analysis, starting from the well-known material parameters and matching conditions.

In the low-field magnetoresistance, lateral superlattices exhibit oscillations which are periodic in the reciprocal magnetic field, $1/B$.[5,6] This behavior can be described in a quasiclassical model,[7] which was generalized by Gerhardts[8] to include higher harmonics. Within this framework, the oscillating contribution $\Delta\rho_{xx}$ to the low-field magnetoresistivity ρ_{xx} is given by

$$\left(\frac{\Delta\rho_{xx}}{\rho_{xx0}}\right)=\sum_{n=1}^{\infty}2n\left(\frac{eV_n}{E_F}\right)^2\left(\frac{l^2}{a^2}\right)B^{\mathrm{res}}\cos^2\left[\pi\left(\frac{n}{B^{\mathrm{res}}}-\frac{1}{4}\right)\right], \quad (1a)$$

$$=\left(\frac{e}{E_F}\right)^2\left(\frac{l^2}{a^2}\right)B^{\mathrm{res}}\left[\sum_{n=0}^{\infty}nV_n^2+\sum_{n=0}^{\infty}nV_n^2\sin\left(n\frac{2\pi}{B^{\mathrm{res}}}\right)\right], \quad (1b)$$

where V_n is the contribution of the nth harmonic to the potential modulation, E_F the Fermi energy, $l=\tau v_F$ the mean free path, and $B^{\mathrm{res}}=a/2R_c$ the rescaled magnetic field given in terms of the superlattice period a and the classical cyclotron radius R_c. From Eq. (1) it can be seen that features at distinct values of B^{res} are repeated again at $1/2*B^{\mathrm{res}}$, $1/3*B^{\mathrm{res}}$, etc. An example of such a ''subharmonic'' replica can be seen in the inset of Fig. 1(d).

From Eq. (1b) it can be seen that the modulus of the coefficients V_n of the potential can be directly deduced from ρ_{xx} through a simple Fourier analysis. It is interesting to note that the situation is analogous to the evaluation of optical, x-ray or electron diffraction spectra, where the intensity reflects the Fourier coefficients of the scattering potential, but the sign of the coefficients cannot be obtained due to loss of phase information. Here, however, the tunable quantity is the *classical* cyclotron radius R_c rather than a wavelength.

The samples are prepared from MBE grown modulation doped AlGaAs/GaAs heterostructures which are capped with a thin layer of $In_xGa_{1-x}As$ [see also Fig. 1(a)]. The InGaAs layer is not lattice matched to the AlGaAs/GaAs heterostructure and will be coherently strained as long as its thickness is below the critical thickness. The amount of strain can be accurately controlled in the MBE process by choice of the mole fraction x and the thickness of the strained layer. In the structure used for this letter, we chose a thickness of 10 nm

[a]Electronic mail: Hannes.Luyken@physik.uni-muenchen.de
[b]Electronic mail: Axel.Lorke@physik.uni-muenchen.de

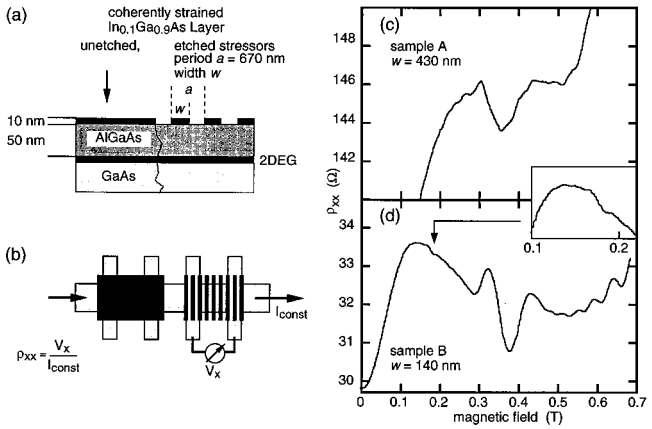

FIG. 1. (a) Schematic of the heterostructure with the InGaAs surface stressor. (b) Hall bar geometry and measuring setup used in the experiment. (c) Longitudinal magnetoresistance ρ_{xx} as a function of magnetic field B for sample A with a stressor width of $w=430$ nm. (d) ρ_{xx} vs B for sample B with a stressor width of $w=140$ nm.

and an Indium content of 10%. This is well below the critical thickness; we estimate the strain in the layer to be $\varepsilon=0.7\%$ assuming Vegard's law. The 2DEG is located 50 nm beneath this strained layer. Hall bars are fabricated by optical lithography and wet chemical etching. Source, drain, and potential probe contacts are provided by evaporated AuGeNi pads, alloyed at 420 °C. *E*-beam lithography and wet chemical etching are employed to define the stressor grating on top of one side of the Hall bar. The other part is left unprocessed to serve as a reference. The period a of our structures is 670 nm, the width w of the stressors is 430 nm in sample A and 140 nm in sample B. After processing, the actual etch depth is determined by atomic force microscopy to 13 nm for sample A and 10 nm for sample B. The four-terminal magnetoresistance across to the grating, ρ_{xx}, is measured at 4.2 K in a standard Hall bar geometry [Fig. 1(b)] with the applied current parallel to the $\langle 110\rangle$ direction. The carrier density and mobility are determined to $N_S=4.2\times10^{11}$ cm^{-2} (sample A), $N_S=5.0\times10^{11}$ cm^{-2} (sample B), and $\mu=4.9\times10^5$ cm^2/V s.

Figures 1(c) and 1(d) show the magnetoresistance ρ_{xx} across the superlattice versus B field. Although the period of the lattice is the same for both structures, the ρ_{xx} traces look quite different, which already indicates the strong influence of the higher harmonics on the effective potential at the location of the 2DEG. For device A, where the stressors are much wider than the spacing in between, we follow the approach used by Deng *et al.*[9] to calculate the conduction band modulation resulting from a one-dimensional stressed superlattice. Starting from standard elasticity theory, the strain components due to the stressors are determined and from there the conduction band modulation. This approach neglects the piezoelectric contributions to the potential modulation (see below).

For the present case, which is homogeneous in the y direction, the energy modulation of the conduction band edge due to strain can be approximated to first order by[10]

$$\Delta E = p(\epsilon_{xx}+\epsilon_{zz}), \tag{2}$$

where p is the hydrostatic deformation potential of the conduction band edge, which can be evaluated from the hydrostatic pressure potential $a'_{\mathrm{GaAs}}=-8.08$ eV to $p=2/3a'$.[11]

It is important to note that both ϵ_{xx} and ϵ_{zz} are linearly dependent on the force per unit length S exerted by the stressor and therefore E, so the actual value of S determines the amplitudes but not the shape of the conduction band modulation. Using the procedure of Ref. 9 and the geometry of sample A, the conduction band modulation is determined as shown in the inset of Fig. 2. The Fourier coefficients of this potential are then determined and used to calculate the longitudinal resistivity ρ_{xx} according to Eq. (1).

In Fig. 2 the calculated curve for ρ_{xx} is shown and compared to the experimental data with a smooth background subtracted.[12] Given the simple analytical ansatz to calculate the strain components, the calculated trace is in good agreement with the experimental data in the relevant regime of magnetic field $0.4\leqslant B_{\mathrm{res}}\leqslant 1.8$ (Below $B^{\mathrm{res}}=0.4$, no oscillations are observed as the mean free path becomes smaller than the corresponding cyclotron parameter; above $B^{\mathrm{res}}=1.8$ there is intermixing between the commensurability oscillations and the Shubnikov de Haas oscillations). The agreement between the experiment and the calculated effect of the deformation potential is an important result, since it is known that strong piezoelectric contributions are present in strained GaAs structures and can even become dominant over contributions of the deformation potential.[13] We cannot completely rule out that in the present structure both contributions coincidentally have a similar shape and are therefore not distinguishable. Evidence of other experiments[3] together with our present findings, however, indicate that the shape of the effective potential follows that of the deformation potential rather than that of the piezoelectric contribution.

It is not possible to apply the same approach to structure B, where the prerequisite that the stressors are much wider than the spacing in between[9] is not fulfilled. A more appropriate way would be a finite element analysis of the strain components, which is beyond the scope of this letter. Instead, we reverse the approach and, using Eq. (1), determine the Fourier coefficients of the effective potential from the resistivity ρ_{xx}. The solid line in Fig. 3 shows ρ_{xx}/B (as determined from the experimental data with a smooth back-

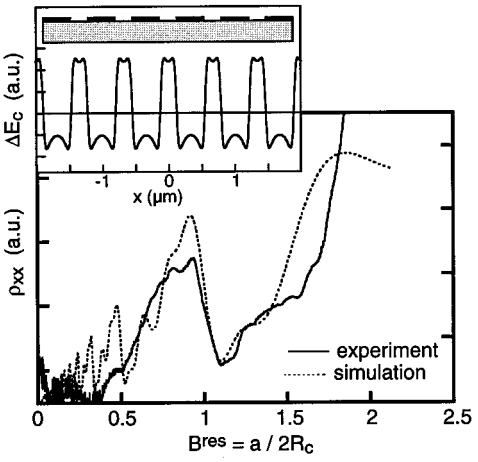

FIG. 2. Solid line: Longitudinal magnetoresistance of device A with a smooth background subtracted. Dotted line: Magnetoresistance as calculated from Eq. (1) with the Fourier components taken from the analytic potential (see inset), derived using the approach by Deng (Ref. 9).

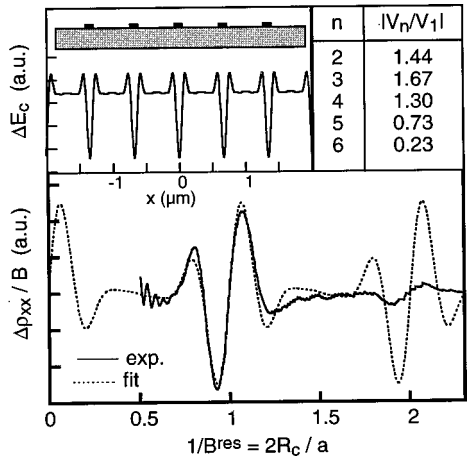

FIG. 3. Solid line: Experimental longitudinal conductivity ρ_{xx}/B plotted against the normalized cyclotron diameter $2R_c$ to allow for a direct comparison with Eq. (1). Dotted line: Fit to the data using Eq. (1) and the Fourier components given in the table. Note that also the higher harmonic structure [arrow in Fig. 1(d)] is reproduced by the fit. Inset: Potential landscape at the location of the 2DEG as constructed from the Fourier components V_n, and compared to the etched stressor structure.

ground subtracted), plotted against $1/B^{\mathrm{res}}$. Note the antisymmetric shape of the experimental data, which already reflects the properties of the Fourier series in Eq. (1b). The large gap between the main structure $(2R_c/a=1)$ and the first subharmonic $(2R_c/a=2)$ already indicates strong contributions from higher harmonics. This is confirmed by a Fourier analysis according to Eq. (1b) (dotted line). In particular, all components up to $n=5$ are stronger than or comparable to the first harmonic (see table in Fig. 3).

In general, the loss of phase information makes it impossible to construct the shape of the lateral potential from such a Fourier analysis. In the present case, where only the first six harmonics give significant contributions, it turns out that only two combinations of signs give potential shapes which are physically meaningful. One of these (with all negative V_n) is shown in the inset in Fig. 3. It is worth noting that this shape reproduces the surface stressor geometry with remarkable accuracy: The distance between the potential maxima as deduced from the transport spectroscopy is 170 nm, in good agreement with the stressor width of 140 nm, as determined from atomic force microscopy (AFM) measurements. The other possible potential modulation (V_1 positive, V_2 through V_6 negative) does not drastically differ from that shown in Fig. 3. The main difference is a well-developed potential minimum between the stressors. The finer features below the stressor, however, are only dependent on the higher harmonics and are therefore indistinguishable from the ones shown in Fig. 3. Our procedure thus allows us to determine in detail the effective potential at the location of the 2DEG, induced by the surface stressor. In principle it is also possible to determine the absolute magnitude of the Fourier coefficients from Eq. (1). From this calculation we obtain a total conduction band modulation of 0.3 meV, which, for the present data, however, has a large margin of error, due to the uncertainty of the exact shape of the subtracted smooth background.[14] For comparison, in photoluminescence (PL) experiments we observe that the PL line of the patterned area of the sample is red-shifted by 1.8 meV against the unpatterned part. The origin of the discrepancy between the optical and transport measurements is not fully understood. It can partly be attributed to the strain-induced valence band modulation and partly to the fact that illumination strongly changes the effective potential modulation as a result of the persistent photoeffect. After illumination at relatively low intensities we find from magnetotransport measurements that the contribution of the first harmonic strongly increases whereas all higher order contributions decrease. After further illumination, the commensurability oscillations eventually vanish completely. We attribute this behavior to a conducting bypass in the donor layer which effectively screens out the strain-induced potential.

In conclusion, we have demonstrated that a heterostructure with a coherently strained InGaAs top layer can be used to create lateral potential modulation with strong contributions of higher harmonics. Furthermore, we have shown that through magnetotransport spectroscopy these harmonics can be determined and used to reconstruct the strain-induced potential modulation for conduction band electrons.

The authors would like to acknowledge valuable technical support by A. Kriele and stimulating discussions with J. H. Davies. This work is supported by the BMBF via Grant No. 01BM623, a Max–Planck research award, and by QUEST, a NSF Science and Technology Center via AFOSR Grant No. F49620-94-1-0158. A.S. acknowledges support through the Alexander von Humboldt foundation.

[1] See, e.g., D. Gershoni, J. S. Weiner, S. N. Chu, G. A. Baraff, J. M. Vandenberg, L. N. Pfeiffer, K. West, R. A. Logan, and T. Tanbun-Ek, Phys. Rev. Lett. **65**, 1631 (1990); K. Kash, B. P. Van der Gaag, D. D. Mahoney, A. S. Gozdz, L. T. Florez, J. P. Harbison, and M. D. Struge, Phys. Rev. Lett. **67**, 1326 (1991).
[2] P. D. Ye, D. Weiss, R. R. Gerhardts, K. von Klitzing, K. Eberl, H. Nickel, and C. T. Foxon, Semicond. Sci. Technol. **10**, 715 (1995).
[3] R. Cusco, M. C. Holland, J. H. Davies, I. A. Larkin, E. Skuras, A. R. Long, and S. P. Beaumont, Surf. Sci. **305**, 643 (1994).
[4] E. Skuras, A. R. Long, I. A. Larkin, J. H. Davies, and M. C. Holland, Appl. Phys. Lett. **70**, 871 (1997).
[5] R. Winkler, J. P. Kotthaus, and K. Ploog, Phys. Rev. Lett. **62**, 1177 (1989).
[6] R. R. Gerhardts, D. Weiss, and K. von Klitzing, Phys. Rev. Lett. **62**, 1173 (1989).
[7] C. W. J. Beenakker, Phys. Rev. Lett. **62**, 2020 (1989).
[8] R. R. Gerhardts, Phys. Rev. B **45**, 3449 (1992).
[9] F. Deng, Q. Z. Li, Z. F. Guan, S. S. Lau, J. M. Redwing, J. Geisz, and T. F. Kuech, J. Appl. Phys. **79**, 1763 (1996).
[10] G. E. Pikus and G. I. Bir, *Symmetry and Strain Induced Effects in Semiconductors* (Wiley, New York, 1974).
[11] Landolt-Börnstein, New Ser. III, Vol. 17/2a (Springer, Berlin 1982).
[12] The shape and physical origin of this smooth background, which is of no relevance for the present evaluation, is discussed, e.g., in R. Menne and R. R. Gerhardts, Phys. Rev. B **57**, 1707 (1998).
[13] I. A. Larkin, J. H. Davies, A. R. Long, and R. Cuscó, Phys. Rev. B **56**, 15 242 (1997).
[14] Note, however, that this uncertainty mainly influences the strength of the first Fourier component, so that the evaluation in Fig. 3 is only little affected.